Published in final edited form as:

J Magn Reson Imaging. 2017 October ; 46(4): 1028–1036. doi:10.1002/jmri.25656.

Apparent Diffusion Coefficient Values May Help Predict Which MRI-Detected High-Risk Breast Lesions Will Upgrade at Surgical Excision

Safia Cheeney, MD[1], **Habib Rahbar, MD**[1], **Brian N. Dontchos, MD**[1], **Sara H. Javid, MD**[2], **Mara H. Rendi**[3], **Savannah C. Partridge, PhD**[1,*]

[1]Department of Radiology, University of Washington, Seattle, Washington, USA;

[2]Department of Surgical Oncology, University of Washington, Seattle, Washington, USA;

[3]Department of Pathology, University of Washington, Seattle, Washington, USA

Abstract

Purpose: To investigate whether diffusion-weighted imaging (DWI) features could assist in determining which high-risk lesions identified on dynamic contrast-enhanced (DCE) magnetic resonance imaging (MRI) and diagnosed on core needle biopsy (CNB) will upgrade to malignancy on surgical excision.

Materials and Methods: This Institutional Review Board (IRB)-approved prospective study included participants with MRI-detected Breast Imaging Reporting and Data System (BI-RADS) 4 or = lesions with high-risk pathology on CNB who underwent surgical excision. Twenty-three high-risk lesions detected on 3T breast MRI in 20 women (average age = 54 ± 9 years) were evaluated, of which six lesions (26%) upgraded to malignancy at surgery. DCE, DWI characteristics, and clinical factors were compared between high-risk lesions that upgraded to malignancy on surgical excision and those that did not. Logistic regression modeling was performed to identify features that optimally predicted upgrade to malignancy, with performance described using area under the receiver operating characteristic curve (AUC).

Results: High-risk lesions that upgraded on excision demonstrated lower apparent diffusion coefficient (ADC) than those that did not (median, 1.08×10^{-3} mm^2/s vs.1.39×10^{-3} mm^2/s, $P = 0.046$), and a trend of greater maximum lesion size (median, 24 mm vs. 8 mm, $P = 0.053$). There were no significant differences in lesion type (mass vs. nonmass enhancement, $P = 1.0$) or kinetic features ($P = 0.78$ for peak initial enhancement; $P = 1.0$ for worst curve type) among the high-risk cohorts. A model incorporating maximum lesion size and ADC provided optimal performance to predict upgrade to malignancy (AUC = 0.89).

Conclusion: ADC and maximum lesion size on MRI show promise for predicting which MRI-detected high-risk lesions will upgrade to malignancy at surgical excision.

Dynamic contrast-enhanced (DCE) magnetic resonance imaging (MRI) is an important imaging tool for the detection and management of breast disease.[1,2] Currently, the American

*Address reprint requests to: S.C.P., 825 Eastlake Ave. East, G2-600, Seattle, WA, 98109. scp3@uw.edu.

College of Radiology (ACR) recommends breast MRI for screening women at high risk of developing breast cancer and for breast cancer staging.[2] Although breast MRI is highly sensitive for detection of breast cancer, specificity remains modest, with benign and malignant pathology presenting with overlapping features on DCE MRI. As a result, nearly all suspicious lesions identified on MRI require core needle biopsy (CNB) in order to determine appropriate clinical management.[3]

While the majority of CNBs prompted by breast MRI yield a clear benign or malignant tissue diagnosis, ~3–21% are classified as high risk by pathology.[4] High-risk lesions represent a wide range of nonmalignant breast pathologies, such as atypical ductal hyperplasia (ADH), lobular carcinoma in situ (LCIS), atypical lobular hyperplasia (ALH), radial scar, and papillary lesions, which may predispose a patient to an increased future risk of developing breast cancer.[4–6] In addition, these lesions have more immediate management implications: 13–57% of high-risk pathologies found on CNB will be upgraded to malignancy at time of surgical excision due to the potential for sampling error on CNB.[4,5,7–9] As a result, surgical excision is the current standard of care for CNB diagnosed high-risk lesions to exclude the presence of occult malignancy. Unfortunately, there are currently no definite imaging or pathologic features that can predict risk of upgrade at excision,[4,8–10] causing many women to undergo unnecessary surgeries.[11]

Diffusion-weighted imaging (DWI) is a noncontrast MRI technique that measures the ability of water to freely diffuse in tissue and has shown promise for differentiating benign from malignant breast lesions by measuring apparent diffusion coefficients (ADCs). Lower ADC values are hypothesized to represent areas of greater cellularity, and multiple studies have demonstrated that malignancies exhibit significantly lower ADC values compared to benign lesions.[12–16] Accordingly, lower ADC values in lesions identified as suspicious on DCE MRI that undergo CNB and reveal high-risk pathology may indicate the presence of underlying malignancy. Thus, we sought to investigate whether DWI can assist in determining which high-risk lesions will upgrade to malignancy upon excisional biopsy.

Materials and Methods

This study was a subanalysis of a larger Institutional Review Board (IRB)-approved and Health Insurance Portability and Accountability Act (HIPPA)-compliant prospective study; all patients gave informed consent. Subjects 18 years or older who underwent 3T breast MRI from October 1, 2010, to December 1, 2013, and who had MRI-detected lesions characterized as Breast Imaging Reporting and Data System (BI-RADS) category 4 or 5 were eligible for the study. Clinical indication for breast MRI included extent of disease evaluation for a known cancer, high-risk screening, and problem-solving. In subjects undergoing MRI to evaluate extent of disease for a recently diagnosed cancer, the eligible study lesion must be distinct from the known/biopsied cancer lesion. Subjects receiving neoadjuvant chemotherapy <6 months prior to the MRI were excluded. The study enrolled 271 women with 357 BI-RADS 4 and 5 lesions diagnosed on DCE MRI, of which 281 lesions in 242 women underwent CNB. CNB was performed under MRI or ultrasound (US) guidance, depending on sonographic visibility. At our institution, MRI-guided biopsy is performed for MRI findings that are either felt to be unlikely to be visible on US (small

masses or foci less than 5 mm and nonmass enhancement [NME]) or findings that are in fact sonographically occult on MRI-directed targeted ultrasound. For US-guided biopsies, a 14G CNB device (Achieve, Becton Dickinson, Franklin Lakes, NJ) was utilized, and at least three cores were obtained. For MRI-guided biopsies, a 9G vacuum-assisted breast biopsy device (ATEC, Hologic, Marlborough, MA) was employed to obtain 6–12 cores of the targeted lesion. High-risk pathology was diagnosed on CNB in 32 lesions in 28 women. For this substudy, only the women with CNB-diagnosed high-risk lesions that underwent subsequent surgical excision were evaluated. The clinical 3T MRI examinations acquired prior to CNB, which included both DCE and DWI scans, were analyzed for this study.

MRI Acquisition

Breast MRIs were performed with a Philips Achieva Tx 3T MRI scanner with a dedicated 16-channel bilateral breast coil (Mammo-Trak, Philips Healthcare, Best, Netherlands). MRI sequences were obtained in the axial orientation and each MRI exam included DWI, T_2-weighted fast spin-echo, T_1-weighted nonfat-suppressed, and T_1-weighted fat-suppressed DCE MRI sequences with one pre-contrast and three postcontrast acquisitions.

DCE MRI was acquired with T_1-weighted fat-suppressed 3D fast gradient echo (eTHRIVE) sequences with parallel imaging technique (sensitivity encoding; SENSE).The following imaging parameters were utilized: repetition time (TR) / echo time (TE): 5.9/3 msec, flip angle: 10°, spatial resolution: 0.5 × 0.5 × 1.3 mm, matrix size: 440 × 660, field of view (FOV): 22 × 33 cm, slice thickness: 1.3 mm, in-plane voxel size: 0.5 mm. Post-contrast sequences were acquired with *k* space centered at ~120, 300, and 480 seconds after contrast injection. The contrast agent administered was 0.1 mmol/kg-body weight gadoteridol (Pro-Hance, Bracco Diagnostics, Milan, Italy).

DWI was performed immediately following DCE imaging using a diffusion-weighted echo-planar imaging sequence with parallel imaging and fat suppression (spectral attenuated inversion recovery; SPAIR) with the following parameters: SENSE reduction factor: 3, averages: 2, TR/TE 5336/61 msec, matrix: 240 × 240, FOV: 36 × 36 cm, section thickness: 5 mm, and gap: 0. Diffusion gradients were applied in six directions with b = 0, 100, and 800 sec/mm^2. Acquisition time was 3 minutes 28 seconds.

MRI Interpretation

Clinical interpretations were performed for all MRI studies by fellowship-trained radiologists specializing in breast imaging. Lesions were assessed using the American College of Radiology (ACR) BI-RADS Breast MRI Lexicon and kinetic features were measured using computer assisted diagnosis (CAD) software (CADstream v. 5.2.7, Merge Healthcare, Chicago, IL). Lesion characteristics including lesion type (mass vs. NME), size, location, kinetic features of peak initial enhancement (defined as percent change in signal intensity at 120 sec postcontrast injection), delayed phase worst curve type (persistent enhancement: 10% or greater increase in signal intensity from 120n 480 sec postcontrast, plateau: less than 10% change in signal intensity, or washout: 10% or greater decrease in signal intensity; where in order of severity washout > plateau > persistent), BI-RADS assessment, and recommendation were recorded at the time of interpretation. These MRI

data and subsequent lesion histopathology were entered into our clinical database and were extracted for the purposes of this study.

DW images were analyzed retrospectively by clinical researchers trained in quantitative analysis of breast MR images, who were blinded to lesion pathology outcomes. DWI measurements were performed using in-house software written in Java language that incorporates open source image analysis tools (ImageJ, National Institutes of Health, Bethesda, MD). ADC maps were first calculated from the DWI images by fitting the signal intensities to the monoexponential equation:

$$ADC = \ln(S_0/S_D)/b$$

in units mm^2/s, where S_D is the signal intensity with diffusion weighting b (100 and 800 s/mm^2) and S_0 is the signal intensity without diffusion weighting (b = 0 s/mm^2). For each lesion detected on DCE MRI, a region of interest (ROI) was drawn free-hand on the corresponding b = 800 s/mm^2 DW image. Intervening adipose and parenchymal tissue voxels could be masked out and excluded from quantitation using an interactive thresholding tool.[17] The ROI was then propagated onto the ADC map and the mean ADC of the nonmasked lesion voxels within the ROI was calculated.

Statistical Analysis

Clinical features (patient age, clinical indication for MRI, pathologic subtype, and biopsy method), DCE features (lesion type, kinetic patterns of enhancement, and maximum lesion size) and ADC values on DWI were compared between high-risk lesions that upgraded to malignancy on final surgical excision and those that did not by Wilcoxon rank sum, Fisher's Exact, or χ^2 test. Uni-variable and multivariable logistic regression modeling was performed to identify features that optimally predicted upgrade to malignancy on surgical excision. For logistic regression models, a log transformation was used to make the maximum lesion size variable more normally distributed. For interpretation purposes, odds ratios (ORs) were calculated using standardized variable values (calculated by subtracting the group mean and dividing by the standard deviation). Model performance was compared by receiver operating characteristic (ROC) curve analysis and calculation of areas under the ROC curves (AUCs). Computations were performed using JMP v. 12.1.0 (SAS, Cary, NC) and R v. 3.2.2 (R Foundation for Statistical Computing, Vienna, Austria). $P < 0.05$ was considered significant for all comparisons.

Results

High-risk pathology was diagnosed on CNB in 32 lesions in 28 women. Of these lesions, one was excluded because DWI was not included in the MRI exam and eight were excluded because definitive final pathology was not available for the following reasons: patient declined excision ($n = 1$), surgery performed at an outside institution and pathology unavailable ($n = 1$), and lesion removed during lumpectomy or mastectomy for a known cancer in ipsilateral breast and final pathology related to that specific lesion could not be confirmed ($n = 6$). Therefore, 23 high-risk lesions in 20 women were included in the study;

two women each had multiple high-risk lesions identified on their MRI examinations. Indication for breast MRI included extent of disease evaluation for a known cancer (11/20), high-risk screening (8/20), and problem-solving (1/20). Patient and lesion characteristics are given in Table 1.

Nineteen lesions (10 masses, 9 NMEs) underwent MRI-guided biopsy while four lesions (three masses, one NME) underwent US-guided biopsy. Eleven (three masses, eight NMEs) of the 19 lesions that underwent MRI-guided biopsy underwent MRI-guided sampling without first performing a targeted ultrasound due to low probability for US detection, while eight were performed under MRI guidance because no sonographic correlate was identified (seven masses, one NME). Surgical excision was performed by excisional biopsy in 18 of 23 lesions, lumpectomy in two, and mastectomy in three (where a pathologic correlate to the biopsied suspicious MRI lesion was reported and/or confirmed for our study by the collaborating pathologist).

Lesion pathologies on CNB included ADH (8/23), lobular neoplasia (LN) such as lobular carcinoma in situ or atypical lobular hyperplasia (13/23), focal atypical apocrine metaplasia (1/23), and radial scar (1/23). Upon surgical excision, 6/23 (26%) lesions upgraded to malignancy: three were determined to be DCIS, two were invasive lobular carcinoma, and one was invasive ductal carcinoma.

Association of Clinical Features With Upgrade

Patient age and clinical indication for MRI (to evaluate extent of a known cancer vs. other indications) were not significantly associated with upgrade ($P = 0.18$ and $P = 0.56$, respectively). Distribution of pathological subtypes that upgraded (50% [3/6] ADH, 50% [3/6] LN) was similar to those that did not (29% [5/17] ADH, 59% [10/17] LN, 12% [2/17] other, $P = 0.41$). Biopsy method was also not significantly different between upgraded and nonupgraded lesions ($P = 0.10$). The six upgraded lesions were all biopsied via MRI vacuum-assisted breast biopsy (VABB) with 9G needles. Of the nonupgraded lesions, 13 were MRI-guided VABB and four were ultrasound-guided biopsies performed with 14G needles.

Association of DCE MRI and DWI Features With Upgrade

DCE and DWI features are reported in Table 2 for lesions that did and did not upgrade at surgery. There were no significant differences in lesion type or kinetic features on DCE MRI between the high-risk lesion groups that did and did not upgrade. Lesion types in the upgraded group included three (50%) masses and three (50%) NMEs. The MRI kinetic features of the upgraded group included median peak initial enhancement of 160% (range, 111–348%), and all exhibited delayed phase worst curve type of washout.

Maximum lesion size, as defined by the longest dimension of the lesion measured on DCE MRI, exhibited a trend of association with lesion upgrade. Lesions that upgraded to malignancy tended to have greater maximum lesion size than those that did not, although the difference did not reach statistical significance. The median lesion size for upgraded lesions was 24 mm (range, 11–97 mm), while the median lesion size for nonupgraded lesions was 8 mm (range, 5–98 mm, $P = 0.053$).

DWI measures of ADC were also associated with lesion upgrade, with high-risk lesions that upgraded to malignancy demonstrating lower ADC compared to the nonupgraded lesions. Upgraded lesions had a median ADC value of 1.08×10^{-3} mm^2/s (range $0.88–1.55 \times 10^{-3}$ mm^2/s), while nonupgraded lesions had a median ADC value of 1.39×10^{-3} mm^2/s (range $0.96–2.13 \times 10^{-3}$ mm^2/s, $P = 0.046$). Examples of high-risk lesions that did and did not upgrade, with corresponding ADC measures, are shown in Figs. 1–3.

Prediction of Upgrade to Malignancy

Multivariable logistic regression modeling incorporating predictors with $P < 0.1$ in univariate analysis identified maximum lesion size ($P = 0.04$) and ADC ($P = 0.007$) to be significant independent predictors of upgrade (Table 3). ROC analysis showed a model combining the two imaging features yielded optimal performance to predict the presence of CNB-occult malignancy with AUC (95% confidence interval [CI]) of 0.89 (0.76, 1.0), which was higher than that of maximum lesion size or ADC alone (AUCs of 0.77[0.58, 0.99] and 0.78 [0.53, 1.0], respectively) (Fig. 4).

Discussion

The number of high-risk lesions diagnosed on CNB is increasing,[18] which presents a clinical challenge due to variable potential for upgrade on surgical excision. In this study of DCE-MRI-detected, CNB-diagnosed high-risk lesions, we evaluated whether DWI features could assist in determining which lesions will upgrade to malignancy on surgical excision. We found that larger lesions with lower ADC values were more likely to upgrade than smaller lesions with higher ADC values. Our results suggest that adding DWI to the standard DCE MRI protocol has potential to assist in decreasing unnecessary surgeries prompted by screening MRIs.

DCE MRI features have previously been studied in the literature in an effort to predict high-risk lesion upgrade risk.[4,6,9,10] In those studies, morphology and kinetic characteristics were not found predictive of lesion upgrade, which agrees with the findings from our study. Furthermore, while we found larger lesions were more likely to upgrade on this study, the prior studies reported no statistically significant association between size and upgrade risk. However, a large retrospective study by Mooney et al evaluating 462 high-risk lesions did find a statistically significant higher rate of upgrade of ADH mass lesions measured as greater than 1 cm on any imaging modality, including MRI.[19] Generally, the relationship between lesion size and risk of upgrade makes intuitive sense due to a greater potential for sampling error by CNB in larger lesions that may be heterogeneous. Thus, further evaluation of the use of lesion size as a predictive marker is warranted in larger cohorts.

We found that lesions that upgraded on surgical excision demonstrated lower ADC values than those that did not. This suggests that DWI provides complementary information to DCE MRI, potentially demonstrating areas of higher cellularity within a lesion. These findings are consistent with multiple prior studies that have shown potential for DWI to differentiate benign from malignant breast lesions. In those studies, malignancies presenting on MRI consistently demonstrated statistically lower ADC values than benign lesions, with optimal thresholds ranging from 1.10×10^{-3} mm^2/s to 1.81×10^{-3} mm^2/s reported in the literature.

[13,14,16,20] Our study adds to promising emerging data on the use of DWI to reduce unnecessary biopsies and surgeries. Specifically, the additional information afforded by DWI could be used during MRI guidance to enhance targeting in order to preferentially biopsy the most aggressive portion of a lesion and thereby decrease sampling error and/or after biopsy to better inform which patients diagnosed with high-risk pathology indeed require surgical excision.

Our study had several limitations. This study was performed at a single institution with a uniform MRI technique in a relatively small sample size. The limited sample size did not allow for testing a greater number of lesion characteristics such as additional morphology (shape, margin, etc.) and texture features. Furthermore, the primary aim was to investigate associations of ADC with presence of malignancy in CNB-diagnosed high-risk lesions and the resulting prediction models for upgrade were exploratory. Thus, validation of these findings in larger, independent cohorts at multiple institutions is needed prior to clinical translation. The slice thickness for our DWI acquisition was 5 mm, which was selected to achieve good signal-to-noise ratio (SNR) and full coverage in a short scan time, but could reduce conspicuity of smaller lesions and more diffuse NME lesions. Higher spatial resolution with thinner slices to reduce partial volume averaging may further improve accuracy for characterization of high-risk lesions on DWI. Our study employed a monoexponential diffusion decay model; more advanced approaches (eg, biexponential intravoxel incoherent motion [IVIM], stretched exponential, and/or kurtosis modeling) to further characterize tissue per-fusion and complexity hold potential to extract more valuable biological information from breast DWI scans and may yield better diagnostic tools. In addition, lesions included in this study were first identified on DCE MRI, and their characteristics on MRI were evaluated prior to biopsy. As a result, the findings from this study cannot be applied to MRIs performed to evaluate high-risk lesions that were identified and/or biopsied on other imaging modalities.

In conclusion, our findings suggest that ADC on DWI could be used in concert with maximum lesion size on MRI to determine which MRI-detected high-risk lesions are at elevated risk for upgrade to malignancy on surgical excision. This indicates that DWI could assist in decreasing the number of unnecessary surgeries women undergo due to indeterminate high-risk pathologies. Further study of this DWI application for both improved MRI-guided targeting and postbiopsy management is warranted to decrease morbidity and anxiety prompted by breast MRIs.

Acknowledgments

Contract grant sponsor: National Institutes of Health (NIH); Contract grant number: R01CA151326; Contract grant sponsor: Radiological Society of North America; Contract grant number: 2014-2016 RSNA Research Scholar Grant; Contract grant sponsor: Safeway Foundation

References

1. Saslow D, Boetes C, Burke W, et al. American Cancer Society guidelines for breast screening with MRI as an adjunct to mammography. CA: Cancer J Clin 2007;57:75–89. [PubMed: 17392385]
2. ACR practice parameter for the performance of contrast-enhanced magnetic resonance imaging (MRI) of the breast. Practice Parameter; Amended 2014 (Resolution 39).

3. DeMartini W, Lehman C, Partridge S. Breast MRI for cancer detection and characterization: a review of evidence-based clinical applications. Acad Radiol 2008;15:408–416. [PubMed: 18342764]
4. Heller SL, Moy L. Imaging features and management of high-risk lesions on contrast-enhanced dynamic breast MRI. AJR Am J Roentgenol 2012;198:249–255. [PubMed: 22268165]
5. Kiluk JV, Acs G, Hoover SJ. High-risk benign breast lesions: current strategies in management. Cancer Control 2007;14:321–329. [PubMed: 17914332]
6. Strigel RM, Eby PR, Demartini WB, et al. Frequency, upgrade rates, and characteristics of high-risk lesions initially identified with breast MRI. AJR Am J Roentgenol 2010;195:792–798. [PubMed: 20729462]
7. Heller SL, Hernandez O, Moy L. Radiologic-pathologic correlation at breast MR imaging: what is the appropriate management for high-risk lesions? Magn Reson Imaging Clin N Am 2013;21:583–599. [PubMed: 23928247]
8. Houssami N, Ciatto S, Ellis I, Ambrogetti D. Underestimation of malignancy of breast core-needle biopsy: concepts and precise overall and category-specific estimates. Cancer 2007;109:487–495. [PubMed: 17186530]
9. Crystal P, Sadaf A, Bukhanov K, McCready D, O'Malley F, Helbich TH. High-risk lesions diagnosed at MRI-guided vacuum-assisted breast biopsy: can underestimation be predicted? Eur Radiol 2011;21:582–589. [PubMed: 20839000]
10. Lourenco AP, Khalil H, Sanford M, Donegan L. High-risk lesions at MRI-guided breast biopsy: frequency and rate of underestimation. AJR Am J Roentgenol 2014;203:682–686. [PubMed: 25148176]
11. Pediconi F, Padula S, Dominelli V, et al. Role of breast MR imaging for predicting malignancy of histologically borderline lesions diagnosed at core needle biopsy: prospective evaluation. Radiology 2010; 257:653–661. [PubMed: 20884914]
12. Ei Khouli RH, Jacobs MA, Mezban SD, et al. Diffusion-weighted imaging improves the diagnostic accuracy of conventional 3.0-T breast MR imaging. Radiology 2010;256:64–73. [PubMed: 20574085]
13. Guo Y, Cai YQ, Cai ZL, et al. Differentiation of clinically benign and malignant breast lesions using diffusion-weighted imaging. J Magn Reson Imaging 2002;16:172–178. [PubMed: 12203765]
14. Marini C, Iacconi C, Giannelli M, Cilotti A, Moretti M, Bartolozzi C. Quantitative diffusion-weighted MR imaging in the differential diagnosis of breast lesion. Eur Radiol 2007;17:2646–2655. [PubMed: 17356840]
15. Partridge SC, Demartini WB, Kurland BF, Eby PR, White SW, Lehman CD. Differential diagnosis of mammographically and clinically occult breast lesions on diffusion-weighted MRI. J Magn Reson Imaging 2010;31:562–570. [PubMed: 20187198]
16. Woodhams R, Matsunaga K, Kan S, et al. ADC mapping of benign and malignant breast tumors. Magn Reson Med Sci 2005;4:35–42. [PubMed: 16127252]
17. Rahbar H, Kurland BF, Olson ML, et al. Diffusion-weighted breast magnetic resonance imaging: a semiautomated voxel selection technique improves interreader reproducibility of apparent diffusion coefficient measurements. J Comput Assist Tomogr 2016;40:428–435. [PubMed: 27192501]
18. Morrow M, Schnitt SJ, Norton L. Current management of lesions associated with an increased risk of breast cancer. Nat Rev Clin Oncol 2015;12:227–238. [PubMed: 25622978]
19. Mooney KL, Bassett LW, Apple SK. Upgrade rates of high-risk breast lesions diagnosed on core needle biopsy: a single-institution experience and literature review. Mod Pathol 2016;29:1471–1484. [PubMed: 27538687]
20. Partridge SC, DeMartini WB, Kurland BF, Eby PR, White SW, Lehman CD. Quantitative diffusion-weighted imaging as an adjunct to conventional breast MRI for improved positive predictive value. AJR Am J Roentgenol 2009;193:1716–1722. [PubMed: 19933670]

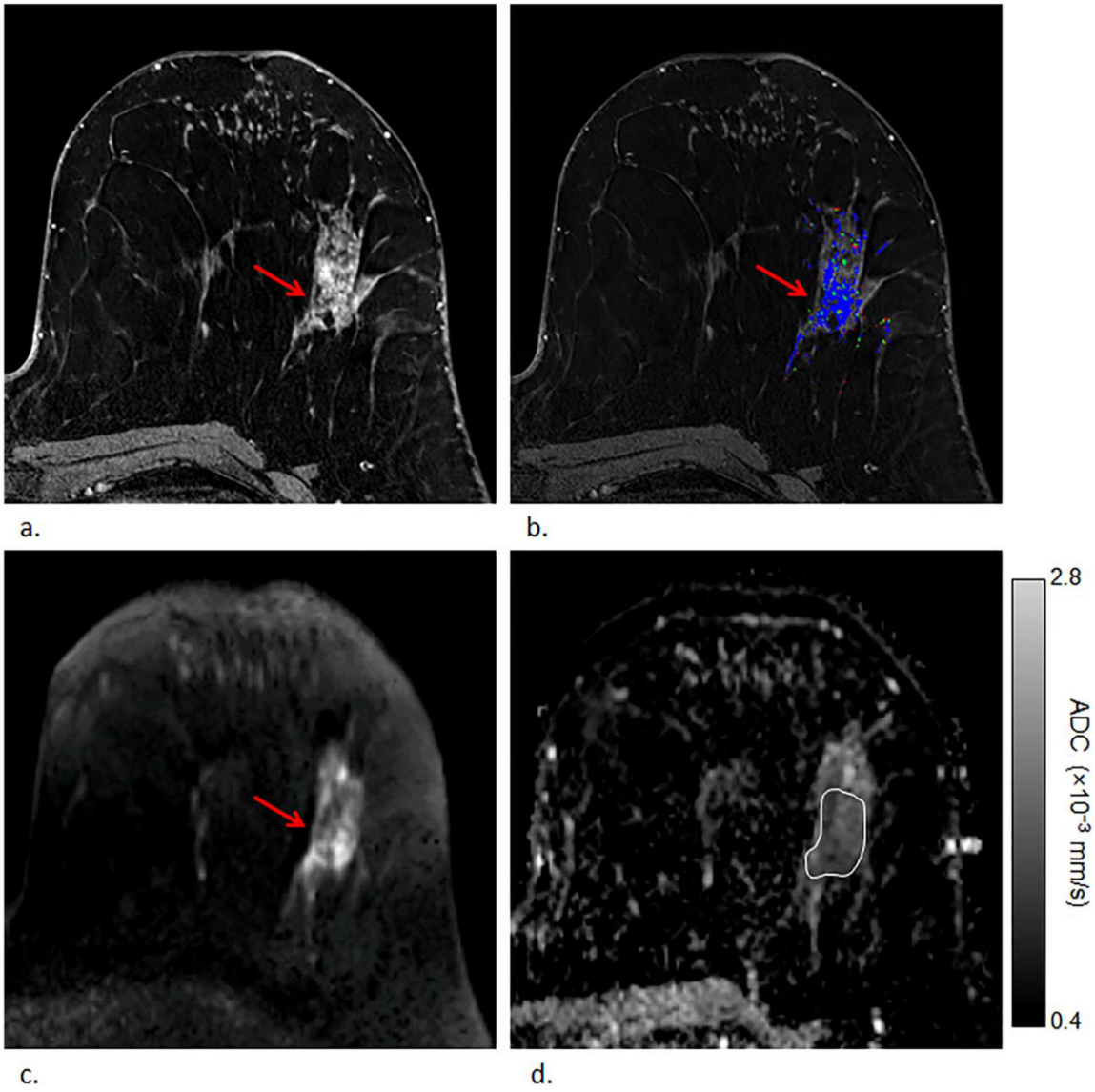

FIGURE 1:

Example of a high-risk lesion (lobular carcinoma in situ) detected in a 54-year-old woman that upgraded to malignancy (ductal carcinoma in situ) on surgical excision. First postcontrast T_1-weighted image (a) and DCE kinetics color map (blue = persistent enhancement, green = plateau enhancement, and red = washout); (b) demonstrates segmental nonmass enhancement in the left breast at 2 o'clock measuring up to 67 mm exhibiting persistent and plateau enhancement that was assessed as BI-RADS category 4. The lesion demonstrated heterogeneously high signal on DWI (b = 800 s/mm^2) (c) with corresponding dark areas on ADC map; (d) with ADC value measuring 1.13 × 10^{-3} mm^2/s.

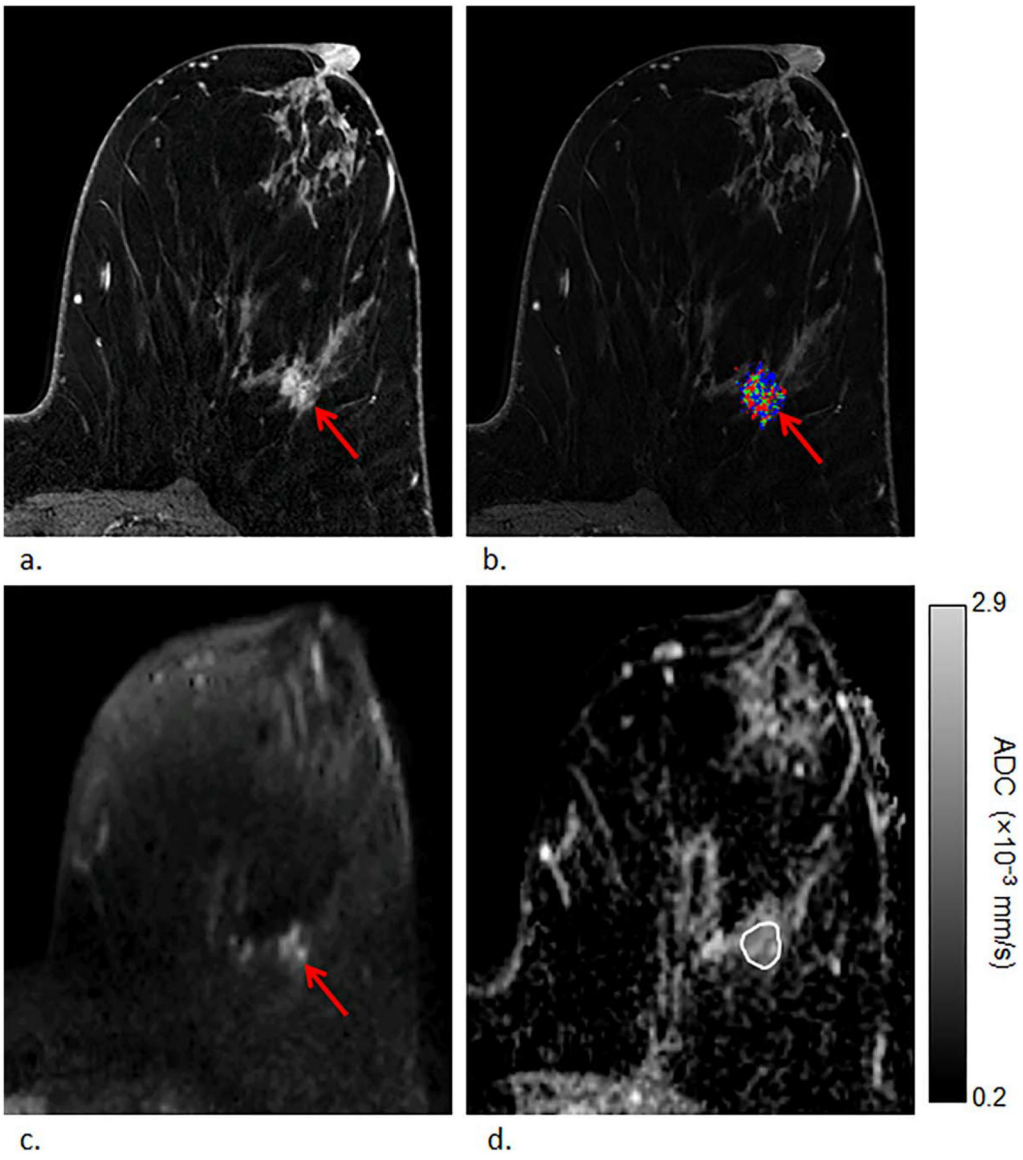

FIGURE 2:

Example of a high-risk lesion (atypical lobular hyperplasia) detected in a 57-year-old woman that remained nonmalignant (lobular carcinoma in situ) on surgical excision, ie, nonupgraded lesion. First postcontrast T_1-weighted image (a) and corresponding DCE kinetics color map (blue = persistent enhancement, green = plateau enhancement, and red = washout); (b) demonstrates nonmass enhancement in the left breast at 3 o'clock measuring up to 15 mm exhibiting washout enhancement that was assessed as BI-RADS category 4. The lesion demonstrated heterogeneously high signal on DWI (b = 800 s/mm^2) (c) with corresponding dark areas on ADC map; (d) with ADC value measuring 1.60 × 10^{-3} mm^2/s.

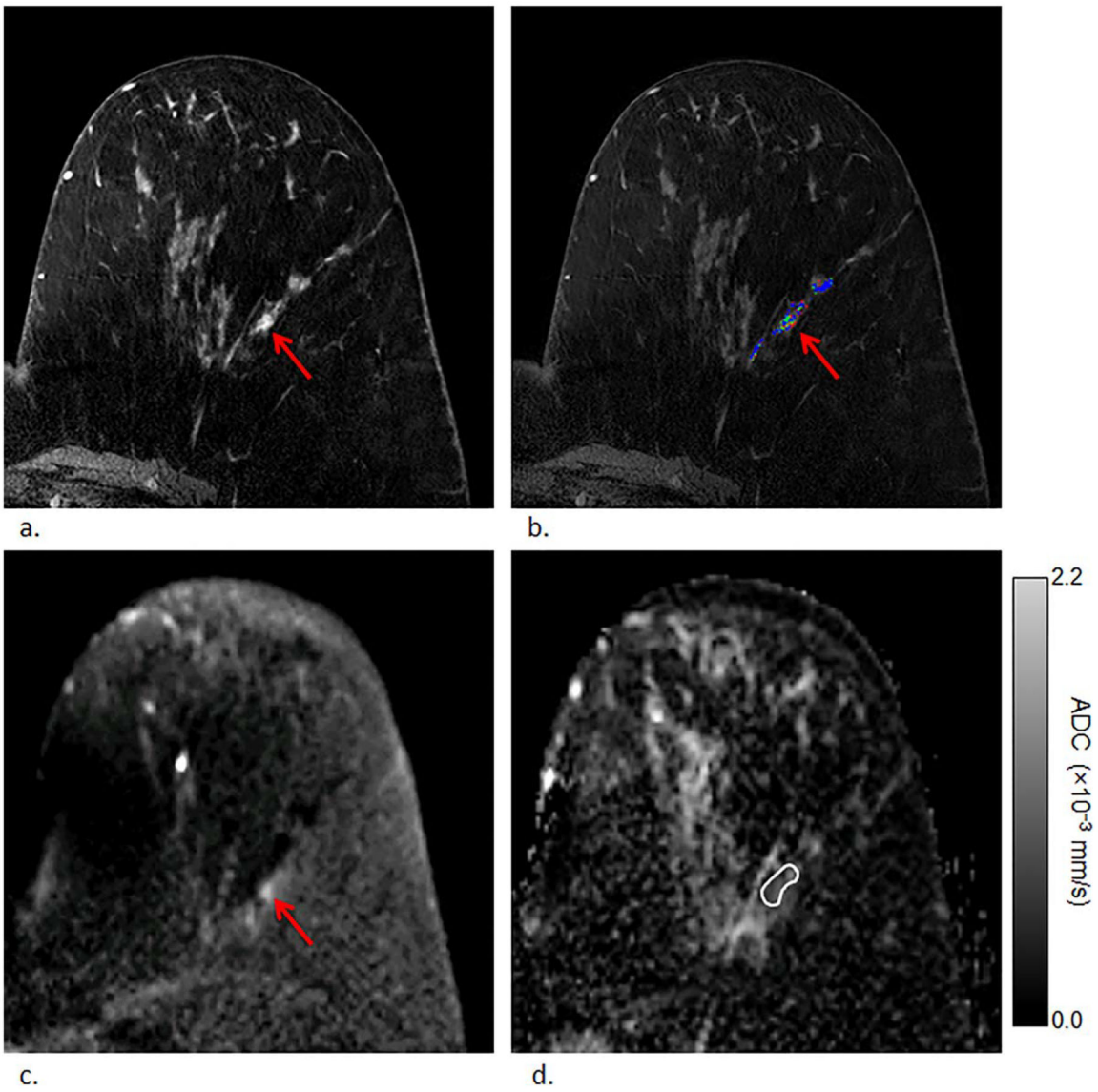

FIGURE 3:

Example of a nonupgraded lesion with low ADC value (atypical lobular hyperplasia that remained nonmalignant lobular carcinoma in situ on surgical excision), detected in a 54-year-old woman. First postcontrast T_1-weighted image (a) and corresponding DCE kinetics color map (blue = persistent enhancement, green = plateau enhancement, and red = washout); (b) demonstrates nonmass enhancement in the left breast at 5 o'clock measuring up to 32 mm exhibiting washout enhancement that was assessed as BI-RADS category 4 (arrow). The lesion demonstrated heterogeneously high signal on DWI (b = 800 s/mm^2) (c) with corresponding dark areas on ADC map; (d) with ADC value measuring 0.96 × 10^{-3} mm^2/s.

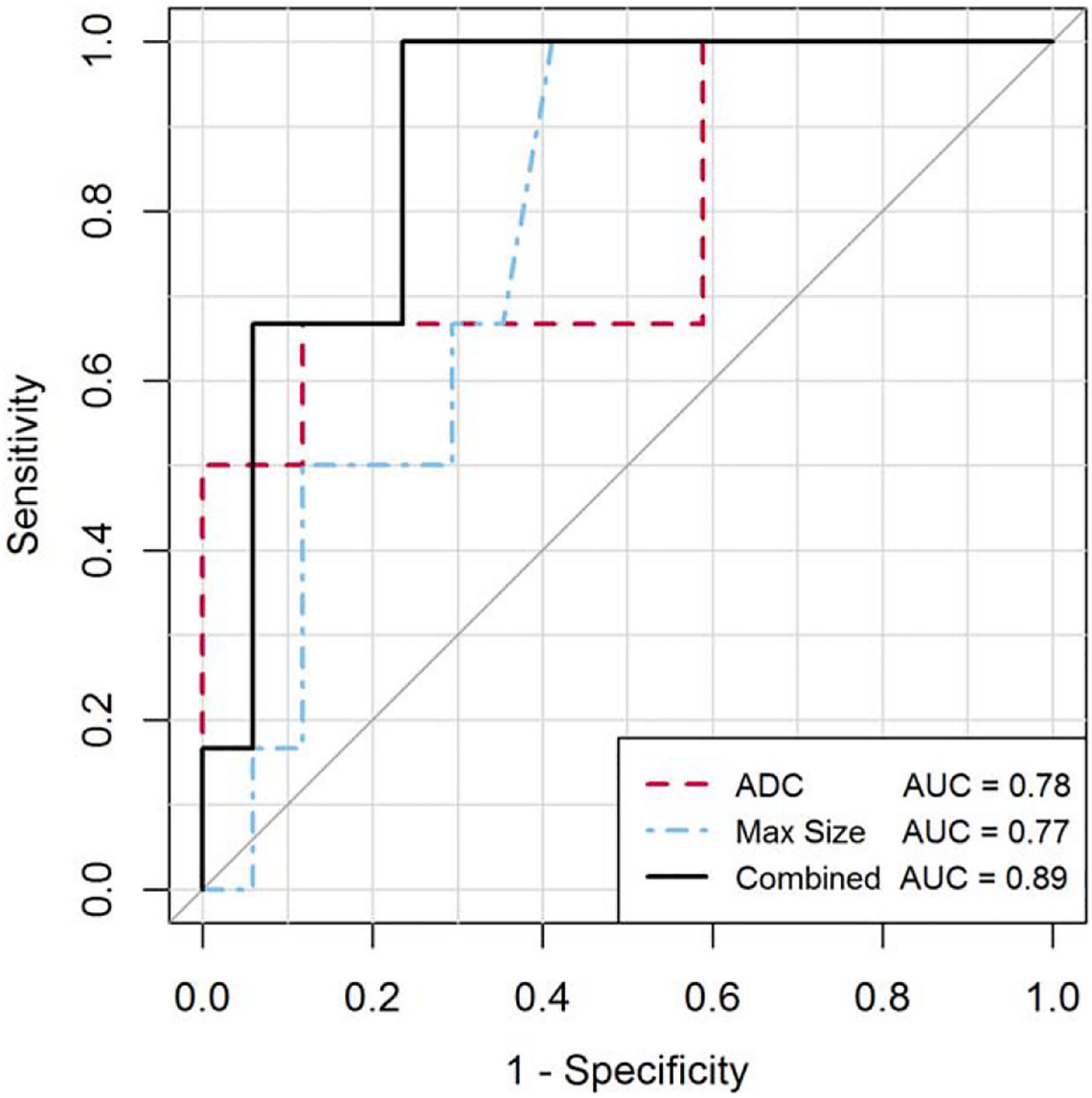

FIGURE 4:

ROC analysis for predicting upgrade to malignancy of CNB-diagnosed high-risk lesions. ROC curves are shown for univariate models of the most predictive imaging features of ADC on DWI and maximum lesion size on DCE MRI and for a multivariable logistic regression model combining the two imaging features using: $y = -2.6 \pm 5.9 \times \text{ADC}$ (units, $\times 10^{-3}$ mm^2/s) – $1.5 \times \log$ [max size] [units, mm]). The combined model significantly differentiated upgrading and nonupgrading lesions with AUC of 0.89 (95% CI, 0.76, 1.0), $P = 0.009$.

J Magn Reson Imaging. Author manuscript; available in PMC 2020 June 01.

TABLE 1.

Patient and Lesion Characteristics

Lesion no.	Patient age (years)	Clinical indication for MRI	Lesion type	BI-RADS	Maximum lesion size (mm)	Biopsy technique	Excision technique	Core needle biopsy diagnosis	Excision diagnosis	ADC value ($\times 10^{-3}$ mm^2/s)
1	64	Screen	Mass	4	5	MRI	Ex	ALH	AAM	1.33
2	63	Known cancer	Mass	4	6	US	Mx	AAM	SA	1.99
3	60	Screen	NME	4	7	MRI	Ex	ADH	SA, UDH	1.67
4	51	Screen	Mass	4	7	US	Ex	ADH	UDH	1.14
5	38	Screen	Mass	4	9	MRI	Lx	LCIS	LCIS	1.62
6	39	Screen	NME	4	22	MRI	Ex	ALH	ALH	1.33
7	47	Known cancer	NME	4	96	MRI	Ex	LCIS	LCIS	1.75
8	54	Known cancer	NME	4	32	US	Ex	ALH	LCIS	0.96
9	57	Known cancer	NME	4	15	MRI	Ex	ALH	LCIS	1.6
10[b]	54	Known cancer	Mass	5	11	MRI	Ex	ADH	UDH	1.34
11[b]	54	Known cancer	Mass	5	7	MRI	Ex	ADH	ALH	1.32
12[b]	54	Known cancer	NME	4	98	MRI	Ex	LCIS	LCIS	1.71
13	54	Screen	Mass	4	8	US	Ex	LCIS	LCIS	1.39
14	43	Screen	Mass	4	12	MRI	Ex	LCIS	LCIS	1.35
15	49	Known cancer	Mass	4	8	MRI	Ex	Radial Scar	ADH	1.48
16	57	Screen	NME	4	7	MRI	Ex	ADH	ADH, SA	1.27
17	54	Known cancer	Mass	4	7	MRI	Ex	ALH	ALH	2.13
18[a]	59	Known cancer	Mass	4	11	MRI	Mx	ADH	DCIS	1.24
19[a]	66	Known cancer	NME	4	35	MRI	Ex	ADH	DCIS	0.88
20[a]	50	Known cancer	NME	4	11	MRI	Lx	LCIS	DCIS	0.92
21[c,a]	69	Problem Solving	Mass	4	13	MRI	Ex	LCIS	ILC	0.91
22[c,a]	69	Problem Solving	NME	4	97	MRI	Ex	LCIS	ILC	1.53
23[a]	38	Known cancer	Mass	4	42	MRI	Mx	ADH	IDC	1.55

[a] Lesions that upgraded to malignant on surgical excision.

[b] Lesions 10, 11, and 12 were detected in a single patient.

[c] Lesions 21 and 22 were detected in a single patient.

AAM, atypical apocrine metaplasia; ADH, atypical ductal hyperplasia; ALH, atypical lobular hyperplasia; Ex, excisional biopsy; IDC, invasive ductal carcinoma; ILC, invasive lobular carcinoma; LCIS, lobular carcinoma in situ; Lx, lumpectomy; Mx, mastectomy; NME, nonmass enhancement; SA, sclerosing adenosis; UDH, usual ductal hyperplasia; US, ultrasound.

TABLE 2.

DCE MRI and DWI Lesion Features

MRI characteristic	Upgraded N = 6 median (range) or *N* (%)	Nonupgraded N = 17 median (range) or *N* (%)	*P* value
DCE lesion type			1.0
mass	3 (50%)	10 (59%)	
NME	3 (50%)	7 (41%)	
DCE kinetics			0.78
Peak enhancement at 120 s (%)	160 (111–348)	199 (105–609)	0.78
Worst curve type			1.0
plateau	0 (0%)	1 (6%)	
washout	6 (100%)	16 (94%)	
Maximum size (mm)	24 (11–97)	8 (5–98)	0.053
ADC ($\times 10^{-3}$ mm^2/s)	1.08 (0.88–1.55)	1.39 (0.96–2.13)	0.046

P-values calculated by Wilcoxon rank sum, Fisher's Exact, or χ^2 test.

DCE, dynamic contrast-enhanced MRI; NME, nonmass enhancement; ADC, apparent diffusion coefficient.

TABLE 3.

Multivariable Logistic Regression Modeling to Predict Upgrade to Malignancy

Variable	OR (CI)	*P* value	Whole model AUC (CI)
ADC	0.15 (0.01–0.65)	0.007	0.89 (0.76–1.0)
Maximum size[a]	3.9 (1.09–23.4)	0.04	

[a]Log(maximum size) used to ensure normality assumption.

Odds ratios expressed are for standardized variables (calculated by subtracting the mean and dividing by the standard deviation). OR, odds ratio of upgrade vs. no upgrade; CI, 95% confidence interval; AUC, area under the ROC curve; ADC, apparent diffusion coefficient.